Improved design approach for silica-based multimode interference devicces

Author/Contributor:
Peng, Gang-Ding; Jin, Zhe

Publication details:
Proceedings of SPIE Volume 5642
pp. 347-354
0819455970 (ISBN)

Event details:
Photonic Asia Conference on Information Optics and Photonics Technology
Beijing, China

Publication Date:
2004

Publisher DOI:
http://dx.doi.org/10.1117/12.580398

Improved design approach for silica-based multimode interference devices

Zhe Jin and Gang-Ding Peng*
Photonics & Optical Communications Group
School of Electrical Engineering & Telecommunications,
University of New South Wales
Sydney 2052, Australia

*g.peng@unsw.edu.au; phone: 0061 2 9385 4014; fax: 0061 2 9385 5993

Abstract

We present an improved design approach for N×N silica-based multimode interference (MMI) devices. By this approach, we could determine a well-defined range of the length of the multimode section that would produce optimal device performance. The range is linked to the propagation constant spacing of fundamental and higher order modes of the multimode waveguide. Related design principles and issues of silica-based MMI devices will be discussed.

Keywords: Multimode interference (MMI) couplers; Optical waveguides; Photonic integrated circuits; Optical signal processing; Silica waveguides

1. Introduction

The multimode interference (MMI) devices have many applications in photonic integrated circuits [1, 2]. The self-imaging theory [1,2] is commonly used to design the devices. Because the theory is based on strongly guided structure if it is applied to design low Δn silica MMI devices that are weakly guided structure the optimal process should be involved [3-5]. In this paper we give an improved approach for the design of silica N×N MMI couplers. Considering the mode propagation constant spacing in the silica multimode waveguide we show that length of MMI section could be adjusted within well-defined ranges to find optimal design of the devices. This approach is applied to design a 4×4 silica MMI couplers, and show that the device width and length must be adjusted simultaneously to get both low loss and good uniformity.

2. N×N MMI Coupler: Model

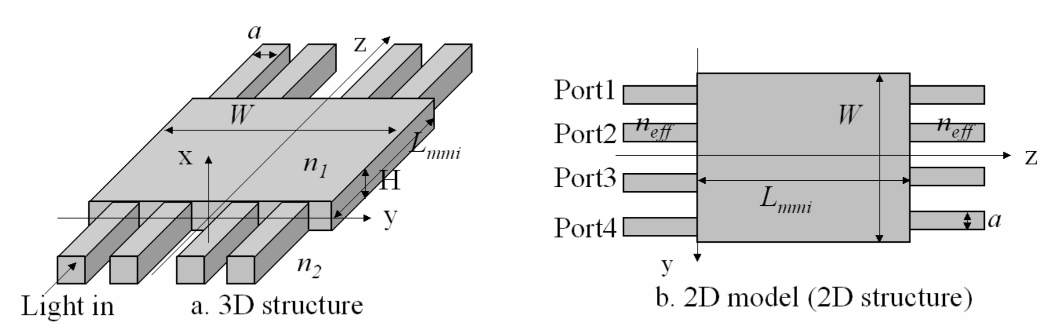

Fig.1. (a) The structure of a silica-based 4×4 MMI coupler and (b) its 2D model.

Information Optics and Photonics Technology, edited by Guoguang Mu,
Francis T. S. Yu, Suganda Jutamulia, Proceedings of SPIE Vol. 5642
(SPIE, Bellingham, WA, 2005) · 0277-786X/05/$15 · doi: 10.1117/12.580398

As shown in Fig.1(a), the central section of a N×N silica MMI coupler (N=4) is a multimode waveguide. In order to launch light into and recover light from this multimode waveguide, a number of access waveguides, usually single-moded, are placed at its beginning and end.

An MMI coupler can be made of silica buried waveguide as reported in [6], with a doped core layer and undoped cladding layers. The transverse direction of the silica waveguide is designed to be single-moded. The effective index method [7] can be used to convert the 3D MMI structure to a simple 2D model [1,2]. As discussed by Chiang in his paper [7], the effective index method solves approximately the scalar wave equation that is accurate for several cases. These cases include arbitrarily shaped waveguides that have a small relative index difference between the core and cladding. The cases here silica waveguides normally have a small relative index difference between the core and cladding and therefore, we would expect good accurate results could be obtained with the method.

Fig.1(b) depicts the 2D model derived from the 3D structure in Fig.1(a). The width and the length of the multimode waveguide are W and L_{mmi}. The core effective index n_{eff} of the correspondent 2D model can be found by the mode index (the propagation constant divided by the free-space wavenumber) in slab along x direction, and the cladding effective index is equal to the cladding index in 3D structure.

3. Self-Imaging Theory

When an input field $\Psi(y,0)$ is injected into the multimode waveguide of an MMI coupler, the guided modes are predominantly excited. Therefore, to good approximation, the input field may be decomposed into the *m* guided modes of the multimode waveguide [1].

$$\Psi(y,0)=\sum_{v=0}^{m-1}c_v\varphi_v(y) \qquad (1)$$

Here, $\varphi_v(y)$ is the νth guided mode. The field excitation coefficients c_v can be estimated using overlap integrals

$$c_v=\frac{\int\Psi(y,0)\varphi_v(y)dy}{\int\varphi_v^2(y)dy} \qquad (2)$$

The field profile at a distance z can then be written as a superposition of all the guided mode field distributions

$$\Psi(y,z)=\sum_{v=0}^{m-1}c_v\varphi_v(y)\exp[j(\omega t-\beta_v z)] \qquad (3)$$

β_v is the propagation constant of the νth eigenmode in the multimode waveguide. Taking the phase of the fundamental mode as a common factor out of the sum, dropping it, and assuming the time dependence $\exp(j\omega t)$ is implicit, the field profile becomes

$$\Psi(y,z)=\sum_{v=0}^{m-1}c_v\varphi_v(y)\exp[j(\beta_0-\beta_v)z] \qquad (4)$$

Using the strongly guided approximation [1, 2], the mode fields amplitudes are given by

$$\varphi_v(y)=\sin(k_{yv}y) \qquad (5)$$

where k_{yv} is the transverse propagation constant of the *v*-th mode. And the propagation constants spacing is

$$\beta_0-\beta_v=\frac{v(v+2)\pi}{3L_\pi} \qquad (6)$$

where

$$L_\pi=\frac{\pi}{\beta_0-\beta_1} \qquad (7)$$

After analysis to Eq. (4) it can be shown [1,2] that there are N images of the input light $\Psi(y,0)$ at

$$z=L_{mmi}=\frac{3L_\pi}{N}. \qquad (8)$$

4. N×N MMI Coupler: Analysis

We now apply guided-mode propagation analysis [1,4] and self-imaging theory to MMI coupler, taking into account the effect of input and output waveguides on loss and uniformity. Also, we take into account in that the 2D structure, TM modes correspond to TE modes in the actual 3D structure. This method is simpler and faster than full modal propagation analysis, and accuracy only slightly compromised.

First the overlap integral of one input field profile and the normalized mode profile of the MMI section is used to find the excitation coefficient when the input field is at the input port. Then the field distributions at the end of the multimode waveguide are calculated. The length of the MMI section is found by Eq. (8). Finally the field coupling into the output waveguides can also be estimated by the overlap integral of the field profile at the end of MMI section and the normalized mode profiles in output waveguides. The loss LS and uniformity UF of a device for one input waveguide port *i* is defined by

$$LS = -10\log_{10}(\sum_j \frac{Pj}{Pin}) \tag{9}$$

$$UF = -10\log_{10}(\frac{Pj\min}{Pj\max}) \tag{10}$$

In our design, the input and output waveguides are positioned symmetrically, as in [3]. These positions are

$$y_j = y_i = \frac{(2i-(N+1))}{2N} We^{(0)} \quad i = j = 1,2,...,N \tag{11}$$

where $We^{(0)}$ is the effective width of fundamental mode, and can be found by

$$We^{(0)} = W + \frac{\lambda}{\pi}(\frac{n_2}{n_{eff}})^{2\sigma}(n_{eff}^2 - n_2^2)^{-(1/2)} \tag{12}$$

λ is wavelength, and $\sigma = 0$ for TE and $\sigma = 1$ for TM. Here we use the effective width $W_e^{(0)}$ instead of the physical width *W* since the modal field is not confined in weakly-guiding waveguides.

We can define a parameter to describe the overall performance of an N×N silica MMI coupler. This parameter is associated with loss (LS) and uniformity (UF) for every input port. We call this parameter the performance (PF)

$$PF = 10^{-\sum_{i'} \frac{UF}{10} - \sum_{i'} \frac{LS}{10}} \tag{13}$$

where $i' = 1,2,..., N/2$ when N is even and $i' = 1,2,...,(N+1)/2$ when N is odd. This definition is similar to that used in [3]. Due to symmetry, summation over all the input ports is not necessary. From Eq. (13) it can be seen that smaller uniformity and loss gives larger performance. The best performance occurs when PF equals 1, and the worst performance when PF is 0.

Using the above analysis we calculate the loss and uniformity for a 4×4 silica MMI coupler in Fig.1. The wavelength is 1.55μm. The refractive indices of core doped silica and cladding silica are 1.46 and 1.456, corresponding to refractive index contrast of $\Delta n = 0.004$, which is the same as single mode fiber [8]. The thickness of the guiding layer and the width of the access waveguides are both 6 μm. The width of multimode waveguide is set as 120um and it is wide enough to prevent coupling between adjacent access waveguides. As mentioned, Eq. (8) is used to find the length of the multimode waveguide. L_{mmi}=14.95mm and the access waveguide position are ± 47.3 μm and ± 15.8 μm When the light is input into port 1 or port 4, the loss and uniformity are determined to be 1.354 dB and 1.048 dB respectively. When light is input in port 2 or port 3, the loss and uniformity are 1.037 dB and 1.696 dB respectively. The performance, PF, of the device is calculated as 0.307. The performance is not particularly good. This confirms that the length determined by the self-image theory is not sufficiently accurate, as reported in [3].

5. Optimizing Design of a Silica N×N MMI Coupler

The reason of low performance is that in silica waveguides the propagation constant spacing is not governed by Eq. (6) and (7). So far if Eq. (8) is still used the images at the output position would have broader peak compared to input field and unwanted ripples, which degrade the performance of the device. Thus we could try to find a new L_π that should make mode propagation constant spacing relation in the silica waveguide fit Eq. (6) better. Substituting this value of L_π into Eq. (8) would give a new L_{mmi}, resulting in better image quality and therefore better performance.

From Eq. (6) L_π can be found by.

$$L_\pi = \frac{v(v+2)\pi}{3\cdot(\beta_0-\beta_v)} \tag{14}$$

In Eq. (14) L_π differs from different mode propagation constant β_v. And it can be transformed to

$$L_\pi(v) = \frac{v(v+2)\pi/k}{3\cdot(\beta_0/k-\beta_v/k)} = \frac{\pi}{3k}\cdot\frac{v(v+2)}{n_{eff\,0}-n_{eff\,v}} \tag{15}$$

In Eq. (15) for every $L_\pi(v)$ $n_{eff\,0}-n_{effv}$ is less than Δn. In silica waveguide normally Δn <<1. But for $v(v+2)$ v is increased by 1. So far we have that $n_{eff\,0}-n_{effv}$ changes little relatively to the changes of $v(v+2)$. Thus as mode index increases $L_\pi(v)$ increases too. This results in a series of $L_\pi(v)$ values, of which the minimum value is given in terms of β_0 and β_1 and the maximum value in terms of β_0 and $\beta_{v\max}$.

$$L_{\pi\min} = L_\pi(1) = \frac{\pi}{\beta_0-\beta_1} \tag{16}$$

$$L_{\pi\max} = L_\pi(v_{\max}) = \frac{v_{\max}(v_{\max}+2)\pi}{3\cdot(\beta_0-\beta_{v_{\max}})} \tag{17}$$

Note that the Eq. (16) is as same as Eq. (7), or the result from self-imagine theory.

The degree of correspondence of mode propagation constant spacings in a silica waveguide to the values given by Eq. (6) with different L_π expressed by Eq. (14) can be checked numerically, and is presented in Fig.2. Here we have introduced a new parameter

$$\Delta_{v\eta} = (\beta_0-\beta_v) - \frac{v(v+2)\pi}{3L_\pi(\eta)} \tag{18}$$

where $\Delta_{v\eta}$ is the difference between the left side and right side of Eq. (6) for every mode propagation constant β_v with different $L_\pi(\eta)$. Certainly $L_\pi(\eta)$ is defined by Eq. (14) with replacing v by η for clear expressions.

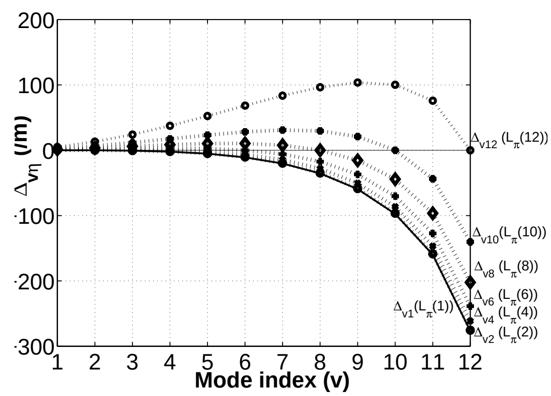

Fig.2. The difference between modal dispersion for a silica waveguide and the ideal dispersion relation given by Eq. (6) with different $L_\pi(\eta)$.

In Fig.2 we use the same parameters as used for the calculation in section 4. For clear presentation on the graph the cases of $L_\pi(\eta)$ found by the two lowest mode propagation constants and by the fundamental mode and even mode propagation constants are given. Looking at Fig.2, it can be seen that the degree to which mode propagation constant spacing in a silica waveguide matches Eq. (6) varies with $L_\pi(\eta)$. The $\Delta_{v\eta}$ is all negative for $L_{\pi\min}$ and the $\Delta_{v\eta}$ is all positive for $L_{\pi\max}$. Better fitting occurs when $L_\pi(\eta)$ is determined from the propagation constants of the fundamental mode and one of the higher modes. This series of values of $L_\pi(\eta)$ results in a series values of L_{mmi} by means of Eq. (8). Using these values of L_{mmi}, loss and uniformity can be calculated to see if better performance can be achieved. Generally it is reasonable to select L_π as a value between $L_{\pi\min}$ and $L_{\pi\max}$. Then L_{mmi} will be in a range

$$L_{mmi\min} = \frac{3L_{\pi\min}}{N} \qquad (19)$$

$$L_{mmi\max} = \frac{3L_{\pi\max}}{N} \qquad (20)$$

Clearly this range is determined by the propagation constants of the fundamental, first, and highest order guided modes. Within this range, we can evaluate the loss and uniformity to find the optimal performance of an MMI device. Note that the min value of the range is as same as the result from self-imaging theory, or Eq. (8). Instead of selecting an arbitrary range near the result from the self-imaging theory as previous approach [3, 4] we show that the length can be adjusted in a range which is found by Eq. (19) and Eq. (20). It is clear that this approach is convenient for finding optimal device length since a well-defined range is given.

The discussion above treats multimode waveguides with a fixed width of W only. However the width of a multimode waveguide also greatly influences the performance of the couplers, and therefore the above analysis must be done for different widths. A new device width will introduce a new series of mode propagation constants and, based on these new propagation constants, a new range of L_π can be found. Thus a new range of L_{mmi} would be determined and used for evaluating the loss and uniformity of the device. In contrast to previous work reported in [3], we optimize the loss and uniformity simultaneously while varying both the width and length of the MMI section.

6. Optimizing of a Silica 4×4 MMI Coupler: An Example

Here we analyze the particular case of a 4×4 silica MMI in order to test our theoretical approach to the design of N×N silica MMI devices. Fig.3 shows the performance parameter, PF, of a 4×4 device for different lengths and widths of the multimode waveguide. We use the same parameters as for our earlier analysis of a non-optimized structure. That is, the wavelength is 1.55μm, the refractive indices of core and cladding are 1.46 and 1.456, and the thickness of the guiding layer and width of the access waveguide are both 6μm.

For different widths of the multimode waveguide, L_{mmi} is varied within the range found using Eq. (19) and Eq. (20). We did calculations for widths of 90μm, 100μm, 110μm, 120μm, 130μm, and 140μm, which correspond to 10, 11, 12, 13, 14, and 15 modes, respectively, in the multimode waveguide. From Fig.3, three different situations occur at different widths. In the first situation, PF changed significantly with device length, and an optimal length could be found in the range given by Eq. (19) and Eq. (20). This situation occurred for widths of 100μm, 120μm, and 130μm. In this situation, we have a new result that there are multiple length/width combinations for which there exists similar optimal performance of the couplers. For example when the width is 120μm and the length is 15.25mm the performance is 0.64, which is similar to the case for which the width is 130μm and the length is 17.64mm. This means that optimal performance can be achieved for several choices of the multimode waveguide size. In the second situation, PF changed slightly and optimal performance could be achieved in the specified range. This situation can be found when the width is 110μm or 140μm. In the third situation, PF changed little in the range and the overall performance is poor. This situation is found when the width is 90μm. In this case, the performance of a device drops slightly and then increases slightly in the specified range. These results show that the width of the multimode waveguide cannot be too small or too large for optimal performance.

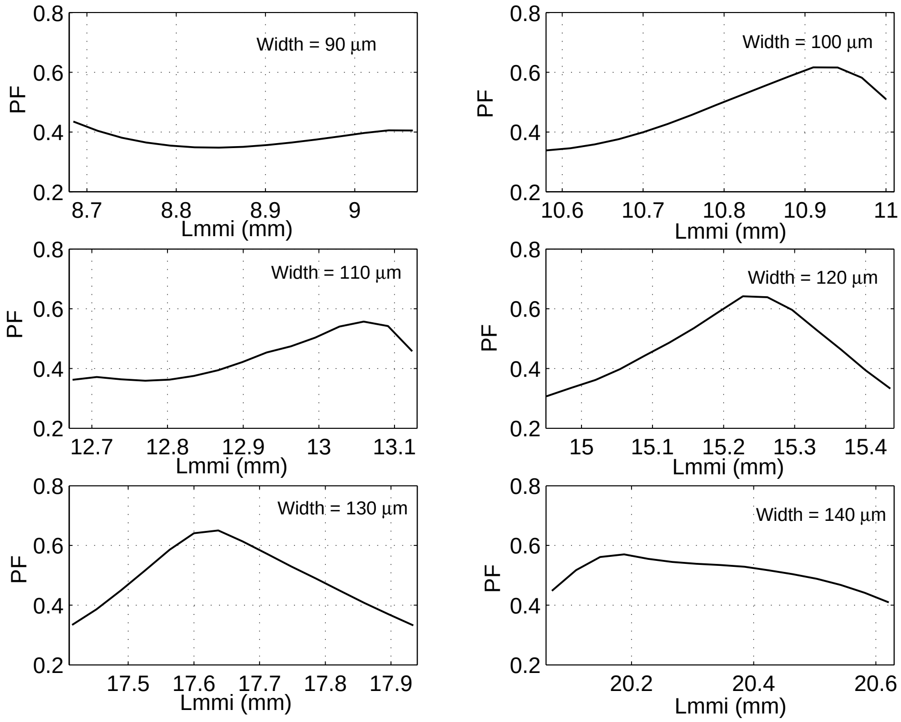

Fig.3. Performance variation for different widths and lengths for a 4×4 MMI coupler.

The performance PF is associated with the loss and uniformity of a device with a number of inputs, and so now we study the loss and uniformity of a device with different lengths and widths to see why in some cases the PF can be improved and in the others it cannot. Figs. 4, 5 and 6 show the detailed features of loss and uniformity versus the length of the multimode waveguide for three width values: 90μm, 120μm, and 140μm. The other parameters are as in Fig.3. These three cases are shown in Fig.3. The length is also optimized in the range determined by the propagation constants of the fundamental, first, and highest order guided modes as calculated using Eq. (19) and Eq. (20).

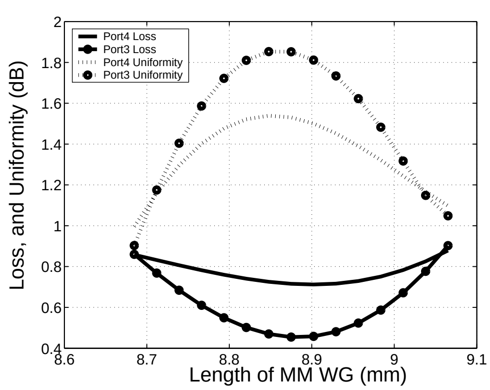

Fig.4 Variation of loss and uniformity with the length of the multimode waveguide
when the width is 90μm

In Fig.4 it can be seen that for every input port the loss is a minimum in the given range, but the uniformity is poor. Since the uniformity exceeds the loss, the performance cannot be improved in this case.

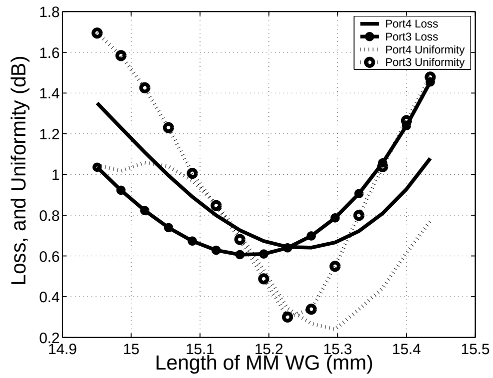

Fig.5. Variation of loss and uniformity with the length of the multimode waveguide when the width is 120μm

In Fig.5 we can see that the loss and uniformity for each input port is a minimum in the given range, and that the optimal positions for both the loss and uniformity of each input port are at similar lengths. Therefore, the performance is significantly better for this width.

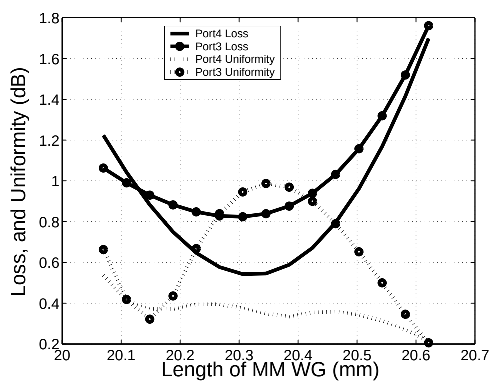

Fig.6 Variation of loss and uniformity with the length of the multimode waveguide when the width is 140μm

In Fig.6 it can be seen that the loss for both input ports is a minimum in the specified range at a length of around 20.35 mm, but the uniformity for port 3 is a maximum at that length. Therefore the overall performance is not significantly improved by adjusting the length within the given range.

From these results, we find that the loss can always be improved within the range but the uniformity has a different behavior. Uniformity improves or deteriorates, depending on the device width. Based on the results, we conclude that if both the loss and uniformity need to be optimized then not only the length but also the width of multimode waveguide should be adjusted. As an example, using the results in Figs. 3-6, an optimal design for both low loss and good uniformity can be found. With the width of multimode waveguide fixed at 120μm, the optimal length is found to be approximately 15.25mm. When we use either port 1 or port 4 as the input, the excess loss and uniformity could be determined to be 0.64 dB and 0.31dB, respectively. Fig.7 shows the relative power intensity distribution at the beginning of the output waveguides. While port 2 or port 3 is used as the input, the loss and uniformity 0.66 dB and 0.33 dB, respectively. Fig.8 shows the relative power intensity distribution at the beginning of the output waveguides The overall performance of this device is 0.64. Comparing the results with the case studied in section 4, where the width and length were not optimized, the value of the performance is improved by more than a factor of 2.

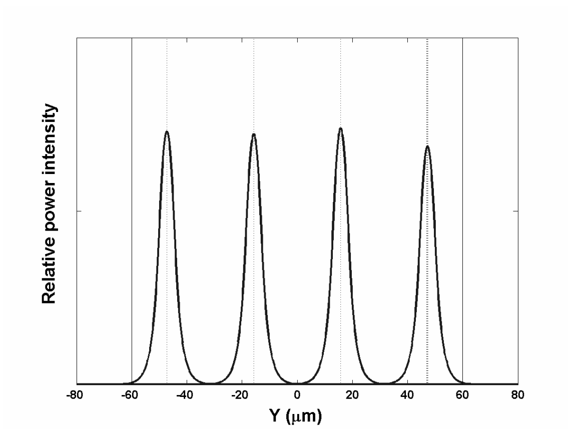

Fig.7 Relative power intensity when port1 is as input for the optimal design of W=120μm

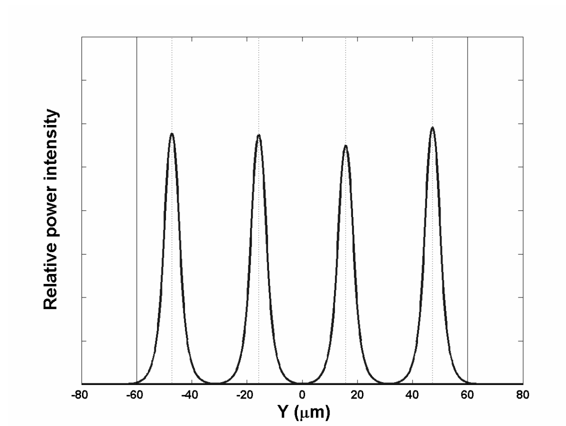

Fig.8 Relative power intensity when port2 is as input for the optimal design of W=120μm

7. Conclusion

In this paper we introduced an improved approach for optimizing the design of silica N×N multimode interference (MMI) couplers. Guided mode propagation analysis was used. The approach adjusts the width and length of the multimode waveguide to achieve optimal device performance. We showed that the length of the multimode waveguide can be varied in a well-defined range to find optimal device performance. This range is related to the propagation constant spacing of the fundamental and higher order modes of the multimode waveguide. We use this approach to optimize the design of a 4×4 silica MMI coupler, and demonstrate that both device width and length must be adjusted to give optimal performance. In the numerical analysis it was found that optimal performance could be achieved for various length/width combinations. Moreover, it was concluded that not only the length but also the width of a N×N silica MMI coupler should be adjusted to achieve both low loss and good uniformity.

8. Acknowledgement

The authors thank Dr. Chris Kaalund for fruitful discussions

9. Reference

1. L. B. Soldano, E.C. M. Pennings, IEEE J. of lightwave tech. Vol.13 No.4 April 1995 P615-627.
2. M. Bachmann, P. A. Besse, H. Melchior, Applied optics, Vol.33 No.18 June 1994 P3905-3911.
3. Q. Wang, J. Lu, S. He, Opt. Commun. 209 (2002) 131-136.
4. T. Rasmussen, J. K. Rasmussen, J. H. Povlsen, J. of lightwave tech. Vol.13 No.10 October 1995 P2069-2074.
5. F. Rooms, A. Morand, I. Schanen, P.Benech, S. Blaize, Opt. Commun. 221 (2003) P317-322
6. L. François, J. D. Love, Silica-based buried channel waveguides and devices, London Chapman & Hall, 1996.
7. Kin S. Chiang, SPIE Vol.2399, June 1995 P2-12.
8. Senior, John M, "Optical fiber communications: principles and practice", 2nd ed. Prentice Hall, 1992